On the Capability and the Future of Parameter Estimation of Compact Binary Coalescence events through measured Gravitational Waves via LIGO, VIRGO, and Cosmic Explorer

Sterling Scarlett*
Valdosta State University,1500 N Patterson St, Valdosta, GA 31698
LIGO Summer Undergraduate Research Fellowship program

Mentors: Alan Weinstein and Jacob Golomb,†
Division of Physics, California Institute of Technology,
1200 E. California Blvd, Pasadena, CA 91125, USA
(Dated: May 8, 2024)

We introduce, understand, and interpret parameter estimation (PE), examining its role in analyzing Compact Binary Coalescence events (CBC) via their emission of Gravitational Waves (GW) and the measured GW strains by instruments such as LIGO and VIRGO. We explain and list all fifteen parameters of CBC. Understanding and looking at current methods of parameter estimations *(Bayesian inference, Fisher Matrix)*, we investigate how each method is currently used *(Bilby)*, future possibilities of the methods via machine learning (Dingo), and advancements in detectors *(Cosmic Explorer)*. Conducting a comparative quantitative analysis considering the speed, accuracy, and precision of the different methods and detectors, we aim to assess their efficiency and capabilities. We focus on simulated high-mass CBC events, allowing us to measure greater accuracy, precision, and characterization of potential strengths and weaknesses of each model and detector.

Keywords: Parameter Estimation, Compact Binary Coalescence, Bayesian Inference, Fisher Matrix, Bilby, Dingo, Cosmic Explorer

I. INTRODUCTION TO *CBC* AND PARAMETER ESTIMATION

Gravitational Waves (GW), predicted by General Relativity and detected by instruments like The Laser Interferometer Gravitational-Wave Observatory (LIGO), offer a window into the universe and provide data for understanding natural phenomena such as compact binary coalescence (CBC). Compact binaries are systems consisting of two compact astronomical objects. Members of this class include binary black holes (BBH), binary neutron stars (BNS), or one of each (NSBH). Coalescence describes all three stages of the collision of compact binaries. First, the objects' decaying orbits draw each other closer until they fully "Inspiral", in which the pair is losing energy and spiraling towards each other. Then they merge into one, producing GW, and lastly, the object stabilizes, forming one body emitting GWs; this stage is called "Ringdown". We therefore define CBC as a system of two compact objects merging, producing GW. These waves carry details about the merging systems, usually binary black holes (BBH), allowing for parameter estimations of the source and resulting black hole [1]. Though compact binaries are the focus of this research, compact mergers are not limited to binaries. There exist different classes of mergers, an example is mergers from hierarchical triple-star systems or triples. These are systems organized as an inner, binary pair with a more distant, outer (tertiary) component [2–4].

Primary mass	m_1
Secondary mass	m_2
Time of coalescence.	t_c
Spin magnitudes	χ_1,χ_2
Sky position	α, δ
Reference phase	ϕ_c
Luminosity distance	d_L
Inclination angle	θ_{JN}
Spin angles	$\theta_1, \theta_2, \phi_{12}, \phi_{JL}$
Polarization angle	ψ

TABLE I. Astrophysical parameters of CBC events.

A. Astronomical parameters of *CBCs*

Focusing on CBC, as shown in TABLE I, the gravitational waveform formed by these events is characterized by fifteen parameters:

- **Detector-frame component masses** (m_1, m_2) - the mass of the larger object involved in the merger (**primary mass** m_1) and mass of the smaller object (**secondary mass** m_2);
- **Time of coalescence** (t_c) - the time when the binary system merges, as measured at the geocenter (center of the Earth);
- **Sky position** (α, δ) - the location of the event on the celestial sphere in right ascension α and declination δ;

* sterling.scarlett3@gmail.com
† ajw@caltech.edu jgolomb@caltech.edu

- **Reference phase** (ϕ_c) - a reference point in the waveform used to describe the phase of the gravitational wave signal at the time of coalescence;
- **Luminosity distance** (d_L) - the distance from the observer to the binary system, calculated based on the observed amplitude of the gravitational wave signal and its intrinsic strength;
- **Inclination angle** (θ_{JN}) - the angle between the total angular momentum vector of the binary system and the line of sight from the observer to the source;
- **Polarization angle** (ψ) - the angle that describes the orientation of the polarization of the gravitational wave signal relative to the line of sight from the observer to the source.
- **Spin magnitudes** (χ_1, χ_2) - the magnitudes of the spins of the two compact objects in the binary system, measured in a 3-vector quantity indicating how fast they are rotating;
- **Spin angles** ($\theta_1, \theta_2, \phi_{12}, \phi_{JL}$) - the various angles that are referenced to the orbital angular momentum $\hat{L}$ and the total angular momentum $\vec{J} = \vec{L} + \vec{S_1} + \vec{S_2}$.

While these fifteen parameters describe CBC, they are not the only quantities that can be measured from GW strain data. Other parameters, derived from the 15 can be defined, such as:

- **Effective Inspiral spin magnitude** (χ_{eff}) - a measurement of the effective spin of the binary system during the "Inspiral" phase, accounting for both individual spins and their orbital orientation, used to find the quantities determining spin parameters;
- **Cosmological redshift** (z) - the stretching of the wavelength of light as it travels through space; determines distance, and can be inferred using d_L;
- **Signal-to-noise ratio** (snr) - measurements of the quantity of strength of the gravitational wave signal compared to the background noise in the detectors;
- **Radiated energy** (E_{rad}) - the energy radiated in GW during the merger;
- **Peak luminosity** (L_{peak}) - the maximum brightness signal emitted;
- **Orbital precession** (δ, ϕ) - the combination of Apsidal precession, where the major axis of an elliptical orbit cycles its orientation within its orbital plane, and Nodal precession, where non-spherical objects cause orbiting objects to change their orbits;
- **Eccentricity** (e) - a measurement of how non-circular the orbit of the final object is;
- **Chirp mass** ($\mathcal{M}_\odot$) - the combination of the two object masses of the system;
- **Final Mass** ($M_\odot$) - the mass of the resulting black hole after the merger.

[5]

Another set of parameters that extends the description (not derived from the 15) specifically for BNS is

- **Tidal distortion parameters** (Λ_1,Λ_2) - These refer to the effects of tidal forces on the shapes and orbits of the neutron stars in the binary system.

.

The parameters of CBCs live in a 15-dimensional space; when making parameter estimations of them in CBC events, detectors such as LIGO, observe and measure the GW strains from the event, take the outputted data space of the strain, and model it in the 15-dimensional space over a function of time $h(t)$. However, there lies the difficulty in visualizing all fifteen parameters. As shown in FIG 1 taken from the LVK collaboration (LIGO, VIRGO and KAGRA) visualization of data measuring the one- and two-dimensional posterior probability distributions for the component masses of the source binary of GW230529, and the one-dimensional (diagonal) and two-dimensional (off-diagonal) marginal posterior distributions for the primary mass m_1, the mass ratio q, and the spin the component parallel to the orbital angular momentum $\chi_{1z} = \vec{\chi_1} \cdot \hat{L}$ [6], scientists tend to limit the visualization to small integer dimensional analysis.

B. Population of events and exceptional events

By analyzing CBC events and conducting parameter estimations, scientists construct distributions of observed mergers, forming populations of events; these populations are used as the foundation for predictive models and simulations of potential future events. FIG 3 shows a population of events developed from confirmed CBC events observed via LIGO, sorted by Final Mass $M_\odot$ to Chirp-mass $\mathcal{M}_\odot$. However as shown in the figure, some observed events deviate from these populations, termed "exceptional events". These expected occurrences, such as black hole mergers resulting in unusually high final masses $M_\odot$, [7] or high component spins χ_1, χ_2 [8], challenge current theoretical frameworks. Presently, the origins and mechanisms behind these events are unknown. However, leading theories suggest scenarios involving hierarchical compact binary coalescence, in which coalescence binary black hole systems merge with another system [9]. A definitive understanding is lacking; leading to uncertain predictability and parameter estimation of these events, prompting our data collection and further

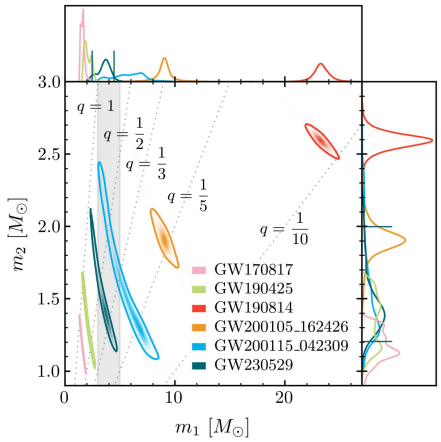

FIG. 1. The one- and two-dimensional posterior probability distributions for the component masses of the source binary of GW230529 (teal). The contours in the main panel denote the 90% credible regions with vertical and horizontal lines in the side panels denoting the 90% credible interval for the marginalized one-dimensional posterior distributions. Also shown are the two O3 NSBH events GW200105 162426 and GW200115 042309 (orange and blue respectively; Abbott et al. 2021a) with FAR < 0.25 yr ≈ 1 (Abbott et al. 2023a), the two confident BNS events GW170817 and GW190425 (pink and green respectively; Abbott et al. 2017a, 2019a, 2020a, 2024b), as well as GW190814 (red; Abbott et al. 2020c, 2024b) where the secondary component may be a black hole or a neutron star. Lines of constant mass ratio are indicated by dotted gray lines. The grey shaded region marks the 3–5 $M_\odot$ range of primary masses. The NSBH events and GW190814 use combined posterior samples assuming a high-spin prior analogous to those presented in this work. The BNS events use high-spin IMRPhenomPv2 NRTidal (Dietrich et al. 2019a) samples [6].

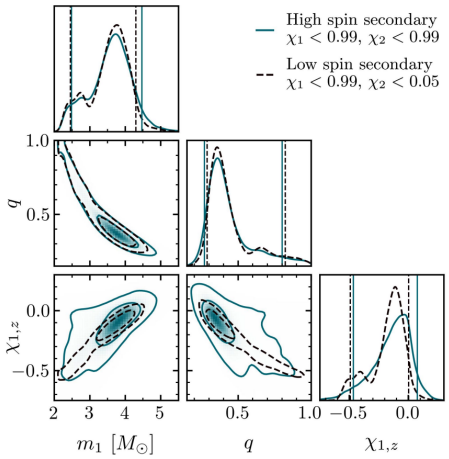

FIG. 2. Selected source properties of GW230529. The plot shows the one-dimensional (diagonal) and two-dimensional (off-diagonal) marginal posterior distributions for the primary mass m_1, the mass ratio q, and the spin component parallel to the orbital angular momentum $\chi_{1z} = \vec{\chi_1} \cdot \hat{L}$. The shaded regions denote the posterior probability with the solid (dashed) curves marking the 50% and 90% credible regions for the posteriors determined using a high spin (low spin) prior on the secondary of $\chi_2 < 0.99$ ($\chi_2 < 0.05$). The vertical lines in the one-dimensional marginal posteriors mark the 90% credible intervals [6].

analysis of them. Addressing this knowledge gap is crucial for advancing our comprehension of accurate estimation of astrophysical processes and the evolution of black hole systems [1].

C. Parameter Estimation Methods

1. *Bayesian inference*

Given a set of parameters $\vec{\theta}$ derived from a prior model and a set of data d, Bayesian inference aims to create a posterior distribution according to Bayes' theorem.

$$p(\theta|d) = \frac{L(d|\theta)\pi(\theta)}{\mathcal{Z}} \tag{1}$$

$p(\theta|d)$ can be interpreted as a conditional probability: the posterior probability distribution (PPD) for θ given the data d; $\mathcal{L}(d|\theta)$ is the probability of getting the data d given a set of model parameters θ. Since the data also

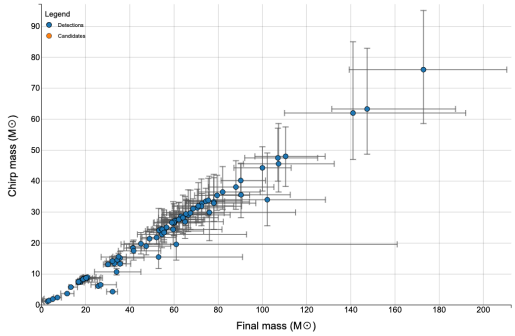

FIG. 3. population distribution of confirmed CBC events via LIGO.

contain gaussian noise: $d = h(t|\theta) + n$, the probability distribution is a gaussian in data space; $\pi(\theta)$ is the prior distribution for θ, and $\mathcal{Z}$ is interpreted as the integral of the numerator or normalization factor called the "evidence" [10].

$$\mathcal{Z} = \int \mathcal{L}(d|\theta)\pi(\theta)d\theta \tag{2}$$

Given that θ is the properties of the source, the efficacy to conduct the posterior distribution is determined by the number of parameters aiming to determine, with larger numbers leading to more imprecise approximations

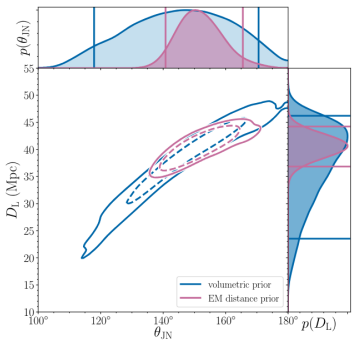

FIG. 4. The joint posterior for luminosity distance and inclination angle for GW170817 from (Abbott et al., 2019). The blue contours show the credible region obtained using gravitational wave data alone. The purple contours show the smaller credible region obtained by employing a relatively narrow prior on distance obtained with electromagnetic measurements. Publicly available posterior samples for this plot are available here: (LIGO/Virgo, LIGO/Virgo) [10].

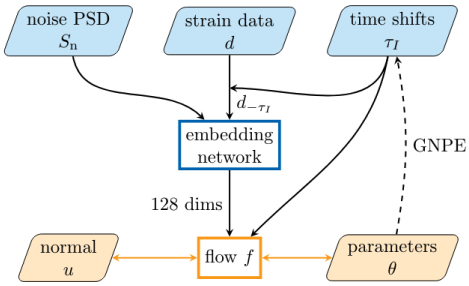

FIG. 5. Dingo flow chart. The posterior distribution is represented in terms of an invertible **normalizing flow** (orange), taking normally distributed random variables u into posterior samples θ. The flow itself depends on a (compressed) representation of the noise properties S_n and the data d, as well as an estimate τ_I of the coalescence time in each detector I. The data are time-shifted by τ_I to simplify the representation. For inference, the iterative *group equivariant neural posterior estimation* (GNPE) algorithm is used to provide an estimate of τ_I, as described in the main text [5].

due to correlation between the parameters. It is noted that leaving out any known parameter when conducting Bayesian Inference leads to a more inaccurate, less precise measurement. This method suffers from "the curse of dimensionality", and is computationally difficult when the source has many parameters such as CBC events. Noting the less accurate nature of the measurement, scientists often construct a **Marginalized posterior distribution** to determine the distribution for a single parameter.

$$p(\theta_i|d) = \int \left(\prod_{k \neq i} d(\theta_k) \right) p(\theta|d) \tag{3}$$

$$p(\theta_i|d) = \frac{\mathcal{L}(d|\theta_i)\pi((\theta_i)}{\mathcal{Z}} \tag{4}$$

This equation can be written in terms of the likelihood function of the specified parameter or **marginalized likelihood function** $\mathcal{L}(d|\theta_i)$.

$$\mathcal{L}(d|\theta_i) = \int \left(\prod_{k \neq i} d(\theta_k) \right) \pi(\theta_k)\mathcal{L}(d|\theta_i) \tag{5}$$

Marginalizing over all but one θ_i results in a 1D posterior distribution on θ_i, which contains all of the uncertainty associated with the other parameters that are covariant with θ_i. An example of this is shown in FIG 4, which shows a marginalized posterior distribution for the well-known covariance between the luminosity distance of a merging compact binary from Earth D_L and the inclination angle θ_{JN} [10].

The previous most common tool used by LVK collaborations for Bayesian inference was LALInference [11]; this code is over a decade old and an updated python-toolkit version of the code has been developed [12]. The successors of these methods, Bilby [13] and Dingo [5] serve as the focus of our research.

a. Bilby is a Python toolkit used to conduct parameter estimation. It sampling of a prior distribution model, to produce a likelihood model using Bayesian Interference. This code has more versatility than its predecessors *(LALInference)*; while mostly used in the estimation of compact binary events [14, 15], it is also used in other astronomical fields such as astrophysical inference in multimessenger astronomy, pulsar timing, and x-ray observations of accreting neutron stars [13]. It serves as not only a more versatile method of Bayesian Interference, but also boasts improvements in efficiency, speed, accuracy, and simplicity over its predecessors [14].

b. Dingo or Deep Inference for Gravitational-wave Observations, is an alternative approach to Bilby. It uses artificial intelligence (AI) machine learning instead of sampling to dramatically decrease the analysis time of gravitational wave inference and parameter estimation of CBC events, at the cost of accuracy and precision. It uses the method of *neural posterior estimation* (NPE) [16, 17], in which it takes large simulated data sets with their associated parameters to train its type of neural network called a *normalizing flow* to produce a posterior distribution, generating distributions quickly after detections' are made, bypassing the need and cost of generating waveform at inference time [5]. A difference in how this method varies from the conventional Bayesian inference methods is how the likelihood is used. Conventional methods such as Bilby use the likelihood to determine density $p(d|\theta)$, while Dingo and NPE methods use the likelihood to simulate data $d \sim p(d|\theta)$ [5].

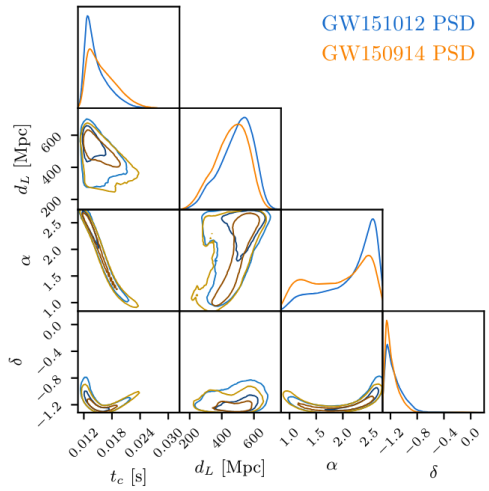

Figure 6. Comparison between DINGO evaluated on GW150914 using correct PSD as context, and using GW151012 PSD. These four parameters have a mean JSD of 0.020 nat.

FIG. 6. Comparison between Dingo evaluated on GW150914 using correct PSD as context, and using GW151012 PSD. These four parameters have a mean JSD of 0.020 nat [5].

2. *Fisher Matrix*

a Fisher matrix or FIM approach is defined as

$$\Gamma_{\kappa\nu} = \left\langle \frac{\partial h}{(\partial\lambda^k)} | \frac{\partial h}{(\partial\lambda^\nu)} \right\rangle = -E\left[\frac{(\partial^2 lnL)}{(\partial\lambda^k\partial\lambda^\nu)}\right] \qquad (6)$$

assumes the waveform measured in CBC events can be seen as a linearizable approximation of the parameters, near enough to the true value, and the error distributions in the parameter errors are Gaussian, meaning the inverse of the FIM is said to give the variance-covariance matrix. Moreover, the square root of the diagonal components of the variance-covariance matrix gives an error estimation in the parameter estimation. As opposed to parameter codes that can produce multi-modal PPDs *(Bilby [13], Dingo [5])*, the FIM approach assumes a mono-modal posterior parameter distribution (PPD), assuming the 15 parameters of the observation describe a 15-dimensional space and the posterior distribution in that space is a 15-dimensional Gaussian with one peak. Rarely is this the case, as shown in both FIG 1 and 4, most events are multi-modal consisting of multiple peaks in their distributions. Therefore the FIM approach is only a rough, fast approximation to the most probable values of the parameters. This approach boasts much faster speeds than Bayesian interference in parameter estimation but suffers greatly in accuracy and precision [18].

II. OBJECTIVES OF RESEARCH

Our primary goal is to conduct a comparative analysis of three parameter estimation methods—*Fisher Matrix*, *Bilby*, and *Dingo*—by employing simulated exceptional events in Python as a benchmark, with a focus on high-mass events. We will also conduct this comparative analysis on the different methods depending on the detector being used to observe the event: *LIGO*, *Cosmic Explorer (CE)*. This comparative study will be done by a quantitative evaluation to discern the efficacy of each method in approximating parameters of interest. In our research, we aim to measure several key aspects:

1. Speed: We will quantify the computational efficiency of each method, particularly focusing on the time taken to generate results of high mass events, and the deviation of the speed depending on varying exceptional events and detectors being used.

2. Accuracy: We will evaluate the accuracy of parameter estimations provided by each model constructed by the scripts. Calculating the percentage error of the known simulated parameter versus the estimated.

3. Capability: We will assess the capability of each of the codes under various conditions, including different degrees of deviation from the observed distribution in simulated events, the number of parameters that each model can handle, the range of parameter space it can handle, and capability between the methods via the detector being used.

It is to be acknowledged that each simulated event deviates from the normal distribution to varying degrees, thereby challenging the efficacy of the coding scripts in accurately capturing these deviations. Additionally, given the intrinsic characteristics of Fisher matrices, we anticipate that although this method offers speed advantages, it will compromise on accuracy compared to other approaches. Furthermore, Dingo claims to be much faster and more efficient than the alternative Bilby [5], therefore significant increases in productivity via Dingo are expected. It is also known that Dingo is only trained on specific simulated events, such as mass ratios from 1:1 to 1:3; it does not have the current capability to construct meaningful distributions for mass relations 1:5 or higher, therefore decreases in the capability of the model in simulated events of this variety are expected. The next-generation detector, CE [19–21], is anticipated to significantly boost the signal-to-noise ratio of observed events. As a result, all parameter estimation methods are expected to show improvements in accuracy and precision.

A. Measures of Successful research

A successful research project will yield several outcomes:

1. Quantitative Insights: We aim to provide quantifiable evidence showing differences among the methods and detectors, offering clear insights into their respective strengths and weaknesses.

2. Advancement Evaluation: Through a detailed analysis, we will assess the extent of improvement introduced by Dingo over its precursor, Bilby, thereby contributing to the evolutionary trajectory of Bayesian interference models. We will also measure the degree of improvement CE has on its predecessor *(LIGO)* in parameter estimation of CBC, providing greater insight into the future of the field.

3. Practical Implications: The findings of our project will have practical implications for researchers and practitioners, aiding them in selecting the most suitable method for their specific applications based on factors such as speed, accuracy, and capability.

By achieving these objectives and criteria for success, we will make substantive contributions to the understanding and advancement of Bayesian interference modeling techniques in the context of exceptional event measurement.

III. APPROACH TO COMPARATIVE ANALYSIS OF METHODS

A. Comparing baseline models:

In Python, we will load both Bilby and Dingo into a Jupyter notebook and download sample data on CBC. Then, we will test each codes' baseline efficiency in determining the known parameters of CBC. This will be done by approximating specific parameters such as binary mass, and comparing it to the known mass, calculating the deviations accrued by each method. Then, we shall increase the number of parameters each code aims to approximate, slowly one at a time, with each increase characterizing the level of deviation of error each method has gained from the previous step. We shall do this for multiple known events multiple times for each event until we have a full collection of baseline data to define each of our methods. Then, we will take comparative numerical data on each of the distribution functions (comparing mean, standard deviation, etc.).

B. Visualizing baseline models:

After comparing models numerically, we will visualize each parameter distribution model we have formed from each code. Comparing each of the parameter distributions to that of our own known simulated distribution. We will see at what points in each distribution the models fail, characterizing the potential weaknesses or strengths of each of the methods.

C. Model enhancement:

Given the nature of the methods of Fisher matrices and Dingo, after preliminary data on strengths and weaknesses, it may be necessary to update parameters in both methods to reflect the weaknesses they exhibit and fine-tune the models. Following this, given that we are focusing on high mass exceptional events and as it has been stated, Dingo has not been fully trained on the full range mass parameters, it will be needed to train Dingo on simulated data to gain more accurate results and comparisons.

D. Parameter estimation of high mass "exceptional" event:

After prior establishment, preliminary data collection, model visualization, and numerical data comparison, we will simulate multiple high-mass exceptional black hole merger events. After measuring the data from each of these events numerically, we will then use all three methods to compute likelihood functions for PE. Using the same format as the preliminary data collection to avoid errors, we will conduct parameter estimation using the likelihood functions derived by each method, initially starting at single parameter estimation, building up to full fifteenth-dimensional approximations, and then calculating error and deviations from actual value in each step.

E. Comparison via methods and events:

Using the found data, we will conduct a qualitative comparative analysis of all three methods, looking at each method separately, delineating where the strengths and weaknesses lie, and measuring the degree of difference in the approximation to that of the simulated distribution. This will be done for each type of event measured for each method. Then a further comparative analysis will be done by relating all findings individually with each method to each other, qualitatively and quantitatively.

F. Comparison via different detectors:

LIGO currently has two detectors, one in Hanford, Washington, and the other in Livingston, Louisiana. Their respective, known performance is well documented,

with their capability and spectral noise curve both respectively known [1, 5–9, 11–17, 22]. CE is a next-generation observatory concept that will greatly deepen and clarify humanity's gravitational-wave view of the cosmos. It will have an L-shaped geometry and house a single interferometer. The CE facility will have two 40 km ultrahigh-vacuum beam tubes, roughly 1 m in diameter, and have two 40 km arms that are 10 times longer than Advanced LIGO, offering the same amplitude of the observed signals but much lower noise, resulting in increases of signal to noise ratio. Being built with all new technology based upon current LIGO technology, the observatory will offer increases in sensitivity and bandwidth of the instruments [19–21].

Estimating the improvement in observations via CE, we will simulate data as if it were detected by the observatory, looking for events at much lower frequencies than LIGO has the means to detect. We will then simulate the same event for the current LIGO observatories and conduct parameter estimation on these events via all three of our methods. This will allow us to show the improvement of parameter estimation via the technological advancements of detectors and offer insight into the changes in efficiency and capability of each parameter estimation method due to different detectors.

IV. PROJECT SCHEDULE

- May 15th - turn in my proposal;
- June 18th: arrive at Caltech campus, moving in with my fellow SURF participants;
- June 18th - meet with my mentors Dr. Alan Weinstein and Jacob Golomb and conduct preliminary parameter estimations;
- June 20th - have my mandatory LIGO SURF orientation;
- July 8-10th - group field trip to the LIGO Hanford Observatory in Richland, WA;
- Late June/early July - turn in my first interim report discussing current progress;
- Early July - learn how to use Fisher matrix with package (Gw fast);
- Late July - turn in my second interim report, reporting possible findings and overall progress on research;
- Early August - finish my research on comparing parameter estimation models;
- Middle of August - revise my abstract and finish the draft of my final report;
- Late August - finish and conduct my oral/paper presentation on my research;
- September-November 1st - finish and turn in the final draft of my research paper.

[1] M. Spera, A. A. Trani, and M. Mencagli, *Compact Binary Coalescences: Astrophysical Processes and Lessons Learned*, Galaxies **10**, 10.3390/galaxies10040076 (2022).

[2] D. R. Czavalinga, T. Mitnyan, S. A. Rappaport, *et al.*, *New compact hierarchical triple system candidates identified using Gaia DR3*, Astronomy & amp; Astrophysics **670**, 10.1051/0004-6361/202245300 (2023).

[3] B. P. Abbott, R. Abbott, T. D. Abbott, *et al.*, *GW190425: Observation of a Compact Binary Coalescence with Total Mass ≈ 3.4 M⊙*, The Astrophysical Journal Letters **892**, L3 (2020).

[4] A. Fabio, T. Silvia, and A. S. Hamers, *Binary Black Hole Mergers from Field Triples: Properties, Rates, and the Impact of Stellar Evolution*, The Astrophysical Journal **841**, 77 (2017).

[5] M. Dax, S. R. Green, J. Gair, *et al.*, *Real-Time Gravitational Wave Science with Neural Posterior Estimation*, Physical Review Letters **127**, 10.1103/physrevlett.127.241103 (2021).

[6] The LIGO Scientific Collaboration, Virgo Collaboration, and the KAGRA Collaboration, *Observation of Gravitational Waves from the Coalescence of a* 2.5 − 4.5 $M_\odot$ *Compact Object and a Neutron Star* (2024), arXiv:2404.04248 [astro-ph.HE].

[7] B. P. Abbott *et al.* (LIGO Scientific Collaboration and Virgo Collaboration), *GW190521: A Binary Black Hole Merger with a Total Mass of 150 M⊙*, Physical Review Letters **125**, 10.1103/physrevlett.125.101102 (2020).

[8] Ng, Thomas C.K. Isi, Maximiliano, Wong, Kaze W.K. *et al.*, *Constraining gravitational wave amplitude birefringence with GWTC-3*, Physical Review D **108**, 10.1103/physrevd.108.084068 (2023).

[9] A. A. Trani, S. Rastello, *et al.*, *Compact object mergers in hierarchical triples from low-mass young star clusters*, Monthly Notices of the Royal Astronomical Society **511**, 1362 (2022), https://academic.oup.com/mnras/article-pdf/511/1/1362/42425280/stac122.pdf.

[10] E. Thrane and C. Talbot, *An introduction to Bayesian inference in gravitational-wave astronomy: Parameter estimation, model selection, and hierarchical models*, Publications of the Astronomical Society of Australia **36**, 10.1017/pasa.2019.2 (2019).

[11] J. Veitch, V. Raymond, B. Farr, *et al.*, *Parameter estimation for compact binaries with ground-based gravitational-wave observations using the LALInference software library*, Phys. Rev. D **91**, 042003 (2015).

[12] C. M. Biwer, C. D. Capano, S. De, *et al.*, *PyCBC Inference: A Python-based Parameter Estimation Toolkit for Compact Binary Coalescence Signals*, Publications of the Astronomical Society of the Pacific **131**, 024503 (2019).

[13] G. Ashton, M. Hübner, P. D. Lasky, *et al.*, *Bilby: A User-friendly Bayesian Inference Library for Gravitational-wave Astronomy*, The Astrophysical Journal Supplement Series **241**, 27 (2019).

[14] C. Hoy and L. K. Nuttall, *BILBY in space: Bayesian inference for transient gravitational-wave signals observed with LISA* (2023), arXiv:2312.13039 [astro-ph.IM].

[15] K. Chandra, A. Pai, S. H. W. Leong, *et al.*, *Impact of Bayesian Priors on the Inferred Masses of Quasi-Circular Intermediate-Mass Black Hole Binaries* (2023), arXiv:2309.01683 [gr-qc].

[16] D. Conor, B. Artur, M. Iain, *et al.*, *Neural Spline Flows* (2019), arXiv:1906.04032 [stat.ML].

[17] G. Papamakarios and I. Murray, *Fast ϵ-free Inference of Simulation Models with Bayesian Conditional Density Estimation* (2018), arXiv:1605.06376 [stat.ML].

[18] M. Vallisneri, *Use and abuse of the Fisher information matrix in the assessment of gravitational-wave parameter-estimation prospects*, Physical Review D **77**, 10.1103/physrevd.77.042001 (2008).

[19] R. Essick, S. Vitale, and M. Evans, *Frequency-dependent responses in third generation gravitational-wave detectors*, Phys. Rev. D **96**, 084004 (2017).

[20] S. Dwyer, D. Sigg, S. W. Ballmer, *et al.*, *Gravitational wave detector with cosmological reach*, Phys. Rev. D **91**, 082001 (2015).

[21] D. Reitze, R. Adhikari, S. Ballmer, *et al.*, *Cosmic Explorer: The U.S. Contribution to Gravitational-Wave Astronomy beyond LIGO* (2019), arXiv:1907.04833 [astro-ph.IM].

[22] B. P. Abbott, A. Abel, C. Charles, *et al.* (LIGO Scientific Collaboration and Virgo Collaboration), *GWTC-3: Compact Binary Coalescences Observed by LIGO and Virgo during the Second Part of the Third Observing Run*, Physical Review X **13**, 10.1103/physrevx.13.041039 (2023).